# UCLA

**Title**

Relative contributions of different sources of epistemic uncertainty on seismic hazard in California

**Permalink**

https://escholarship.org/uc/item/20q0x2hf

**Authors**

O'Donnell, Timothy

Stewart, Jonathan P

Milner, Kevin R

**Publication Date**

2024-07-01

Peer reviewed

18TH WORLD CONFERENCE ON EARTHQUAKE ENGINEERING

WCEE2024
MILAN

MILAN, ITALY
30TH JUNE – 5TH JULY 2024

www.wcee2024.it

# RELATIVE CONTRIBUTIONS OF DIFFERENT SOURCES OF EPISTEMIC UNCERTAINTY ON SEISMIC HAZARD IN CALIFORNIA

T.M. O'Donnell[1], J.P. Stewart[2] & K.R. Milner[3]

[1] Ph.D. Candidate, UCLA Samueli Engineering, Los Angeles, CA, USA, tmo32@g.ucla.edu

[2] Professor, UCLA Samueli Engineering, Los Angeles, CA, USA

[3] Computer Scientist, Statewide California Earthquake Center, University of Southern California, Los Angeles, CA, USA

**Abstract**:  *We evaluate the relative impact of three sources of epistemic uncertainty on probabilistic seismic hazard analyses in California: source model uncertainty, ground motion model (GMM) uncertainty, and site parameter uncertainty. Seismic source model uncertainty is inherently contained in the source model framework applied by the USGS in the 2023 National Seismic Hazard Model (NSHM23); we have added tools to extract this uncertainty for California sites in the open-source seismic hazard software OpenSHA. GMM uncertainty is generally accounted for using alternative models in PSHA or a single backbone model with a defined uncertainty. Site parameter uncertainty refers to uncertainty in the shear wave velocity of the upper 30 meters of the site profile ($V_{S30}$) and potentially other independent site parameters.*

*We demonstrate the impacts of these major sources of epistemic uncertainty at the sites of two UC campuses, Berkeley, which is located near the active Hayward fault, and Davis, which is located in the relatively quiescent Central Valley. We investigate potential correlations between the different sources of uncertainty and find that source uncertainty is practically independent of GMM and $V_{S30}$ uncertainty at Berkeley but dependent on GMM and $V_{S30}$ at Davis. At both locations, GMM and site parameter uncertainty are correlated (i.e., inter-dependent). We represent epistemic uncertainty in ground motion with a period-dependent log-normal standard deviation term that is specific to a given site location, site condition, and exceedance frequency. We show that at Berkeley, the total epistemic uncertainty can be well approximated by the square root sum of squares (SRSS) of source uncertainty (i.e., uncertainty in ground motions related solely to the source model) and the combined GMM and site parameter uncertainty. We find that combined GMM and $V_{S30}$ uncertainty is comparable to or greater than the source uncertainty at many oscillator periods at both sites. Combined uncertainties range from natural log standard deviations of about 0.2 at short periods to 0.6 at Berkeley and 0.3-0.7 at Davis at long periods.*

*Keywords: Epistemic uncertainty, source model uncertainty, OpenSHA, NSHM23, UCERF3*

## 1. Introduction

Two broad classes of uncertainty affect seismic hazard modeling: Epistemic uncertainty and aleatory variability. Epistemic uncertainty results from a lack of knowledge and aleatory variability results from inherent randomness in a physical process that cannot be reduced with additional knowledge (Pate-Cornell 1996, Bommer 2005, Faber 2005, Der Kiureghian and Ditlevson 2009, and Stafford 2015). In probabilistic seismic hazard analysis (PSHA), there is epistemic uncertainty associated with both the ground motions models (GMMs) and source models used to generate hazard curves. This is because both GMMs and source models are developed from limited data that does not fully constrain the models over the required parameter space. For example, GMMs are largely developed using data from moderate to small magnitude earthquakes but are applied in hazard calculations for large-magnitude and often close-distance conditions – the limited knowledge associated with these extrapolations is a major source of epistemic uncertainty. Likewise, seismic source models are developed from mapped (generally visible at the ground surface) faults and a limited (approximately 100 years) record of seismicity; earthquakes can happen on previously unmapped faults and can involve complex series of fault segments that might not have been anticipated pre-event. The manner in which these different rupture scenarios, and their rates of occurrence in time, are modelled is highly uncertain.

Traditionally, epistemic uncertainty is considered in hazard analyses by considering alternative models or alternative parametric inputs into models with corresponding weights using a logic tree approach (McGuire 2004, Bommer et al. 2005). Hazard analyses are performed using each combination of models, thus producing many hazard curves, each with their own weight. The mean hazard that is derived from this process is often used for design purposes (McGuire et al. 2005). If the hazard curves follow a log-normal distribution, the mean hazard can be represented as:

$$\overline{\lambda}_{IM} = exp\left(\mu_{ln\,\lambda} + \frac{\sigma_{ln\lambda}^2}{2}\right) \tag{1}$$

where $\overline{\lambda}_{IM}$ is the mean rate of exceedance of an intensity measure and $\mu_{ln\,\lambda}$ and $\sigma_{ln\,\lambda}^2$ are the median and variance (sampling across the range of results from epistemic uncertainty). The choice of the mean is motivated in part by its sensitivity to the spread of results as shown in Eq. 1.

The goals of this work are to (1) develop tools to facilitate practical means by which source-related epistemic uncertainty can be accounted for in seismic hazard analyses for California sites and (2) evaluate the relative contributions of the major sources of epistemic uncertainty. Quantifying the relative contributions of each individual source of uncertainty is useful for demonstrating where resources should be directed to reduce uncertainties in hazard curves.

The major sources of epistemic uncertainty that are considered are:

1. Source Model Uncertainty
2. Ground Motion Model (GMM) Uncertainty
3. Site Parameter Uncertainty

As shown subsequently, the effects of these uncertainties produce approximately log-normal ground motion distributions. As such, ln standard deviations can be assigned to each source, which are denoted $\sigma_S$, $\sigma_{GMM}$, and $\sigma_{Vs}$, respectively.

Ground motion hazard calculations are performed considering the above uncertainties for a range of return periods. The results are checked to investigate potential correlations between the effects of different uncertainties. Subsequent sections present specific features of the analyses, describe how uncertainties in model components were defined, and present the results.

## 2. Locations, Site Parameters, and Analysis Tools for Hazard Calculations

The quantification of epistemic uncertainty is location-specific. We select two sites that reflect different seismo-tectonic conditions in California. As shown in Figure 1, the UC Berkeley site is located adjacent to a major active fault (Hayward Fault) and is 30 km away from the San Andreas Fault plate boundary. The UC Davis site, while still in a region classified as an active tectonic region, is relative far from the plate boundary faults (105 km from San Andreas) and has no immediately adjacent mapped Quaternary faults.
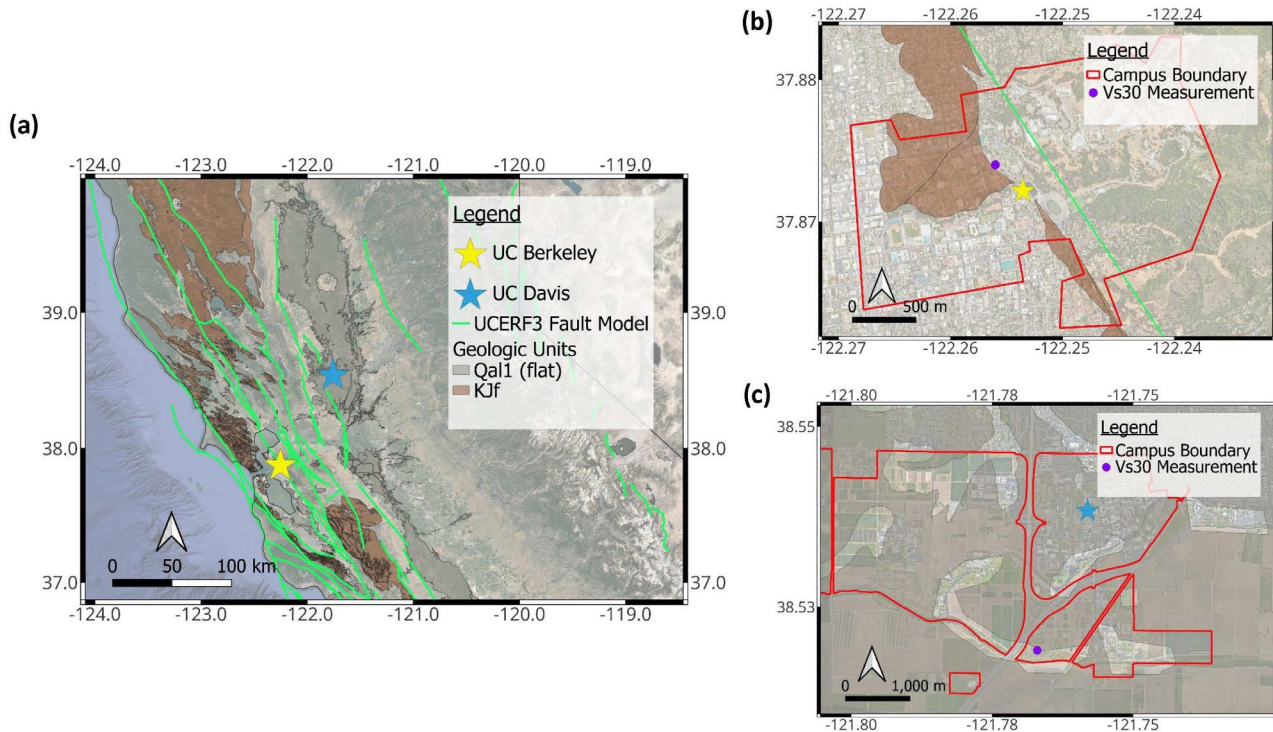
*Figure 1. (a) Locations of UC Berkeley and UC Davis used for analysis along with UCERF3 Fault Models 3.1 and 3.2 and relevant geologic units, Quaternary Alluvium (Qal1(flat)) and Franciscan Complex Rock (KJf) (b) Close up of UC Berkeley and (c) UC Davis campuses with campus boundaries and locations of Vs30 measurements used for analysis.*

The source model used for most recent applications in California has been the Third Uniform California Earthquake Forecast (UCERF3; Field et al. 2014, 2017). For the development of the 2023 National Seismic Hazard Model (NSHM23), the source model has been updated (Field et al. 2023; Milner and Field 2023) in a manner that more accurately captures uncertainties in fault event rates and connectivity. Our selection of the two target sites was intended to produce different levels of source model uncertainty. The UC Berkeley site was expected to have lower source model uncertainties as the site is close to known seismic sources (namely the Hayward fault) with a relatively well constrained geometry and rupture history (Waldhauser and Ellsworth, 2002). The UC Davis site was expected to have higher source model uncertainty as it is relatively far from high-activity mapped faults and thus might be expected to be strongly influenced by relatively poorly constrained faults near the western boundary of the Central Valley and background seismicity, which were expected to be more uncertain.

The site parameter used for analysis is the time-averaged shear wave velocity in the upper 30 meters of the site, $V_{S30}$. For each site, 14 $V_{S30}$ values were used to calculate hazards. Seven representing a distribution appropriate for measured $V_{S30}$ values (small uncertainty) and seven representing distributions appropriate for inferred $V_{S30}$ values (large uncertainty). This was done so that the effects of different levels of site parameter uncertainty could be investigated. The values within each set of seven correspond to percentiles considered optimal for approximating a cumulative distribution function using Gaussian quadrature (Miller and Rice, 1983). The mean value of each set was obtained from site investigation data. The mean $V_{S30}$ for UC Berkeley was acquired from a geotechnical investigation performed as part of a campus-wide seismic hazard study (URS, 2015). The mean $V_{S30}$ for UC Davis was based on a shallow shear wave velocity measurement obtained from a report titled "Phase 1 Geotechnical Data Report (P1GDR): Davis Study Area, Urban Levee Geotechnical Evaluations Program, September 2008". Both $V_S$ profiles were retrieved from the shear wave velocity database (Kwak et al. 2021). When the Vs profile did not extend to 30 m, the model proposed by Dai et al. (2013) was used to estimate $V_{S30}$ based on the shallow measurement (Kwak et al., 2017). The inferred $V_{S30}$ for both the Berkeley and Davis sites were obtained from correlations with surface geology and ground slope, which include natural log standard deviations (Wills et al., 2015). For the measured $V_{S30}$, the natural log standard deviation was taken as 0.1. Table 1 summarizes the $V_{S30}$ values used.

*Table 1. V$_{S30}$ values used to calculate hazards and site parameter uncertainty.*

| Site | Measured or Inferred | Number within set | InSD | Mean Vs30 (m/s) | Percentile | Z-score | Vs30 Value (m/s) |
|---|---|---|---|---|---|---|---|
| UC Berkeley | Measured | 1 | 0.1 | 633 | 0.019 | -2.075 | 514 |
| UC Berkeley | Measured | 2 | 0.1 | 633 | 0.115 | -1.194 | 562 |
| UC Berkeley | Measured | 3 | 0.1 | 633 | 0.285 | -0.567 | 598 |
| UC Berkeley | Measured | 4 | 0.1 | 633 | 0.500 | 0 | 633 |
| UC Berkeley | Measured | 5 | 0.1 | 633 | 0.715 | 0.567 | 670 |
| UC Berkeley | Measured | 6 | 0.1 | 633 | 0.885 | 1.194 | 713 |
| UC Berkeley | Measured | 7 | 0.1 | 633 | 0.981 | 2.075 | 779 |
| UC Berkeley | Inferred | 1 | 0.38 | 633 | 0.019 | -2.075 | 288 |
| UC Berkeley | Inferred | 2 | 0.38 | 633 | 0.115 | -1.194 | 402 |
| UC Berkeley | Inferred | 3 | 0.38 | 633 | 0.285 | -0.567 | 510 |
| UC Berkeley | Inferred | 4 | 0.38 | 633 | 0.500 | 0 | 633 |
| UC Berkeley | Inferred | 5 | 0.38 | 633 | 0.715 | 0.567 | 785 |
| UC Berkeley | Inferred | 6 | 0.38 | 633 | 0.885 | 1.194 | 996 |
| UC Berkeley | Inferred | 7 | 0.38 | 633 | 0.981 | 2.075 | 1393 |
| UC Davis | Measured | 1 | 0.1 | 266 | 0.019 | -2.075 | 216 |
| UC Davis | Measured | 2 | 0.1 | 266 | 0.115 | -1.194 | 236 |
| UC Davis | Measured | 3 | 0.1 | 266 | 0.285 | -0.567 | 251 |
| UC Davis | Measured | 4 | 0.1 | 266 | 0.500 | 0 | 266 |
| UC Davis | Measured | 5 | 0.1 | 266 | 0.715 | 0.567 | 281 |
| UC Davis | Measured | 6 | 0.1 | 266 | 0.885 | 1.194 | 299 |
| UC Davis | Measured | 7 | 0.1 | 266 | 0.981 | 2.075 | 327 |
| UC Davis | Inferred | 1 | 0.19 | 266 | 0.019 | -2.075 | 179 |
| UC Davis | Inferred | 2 | 0.19 | 266 | 0.115 | -1.194 | 212 |
| UC Davis | Inferred | 3 | 0.19 | 266 | 0.285 | -0.567 | 238 |
| UC Davis | Inferred | 4 | 0.19 | 266 | 0.500 | 0 | 266 |
| UC Davis | Inferred | 5 | 0.19 | 266 | 0.715 | 0.567 | 296 |
| UC Davis | Inferred | 6 | 0.19 | 266 | 0.885 | 1.194 | 333 |
| UC Davis | Inferred | 7 | 0.19 | 266 | 0.981 | 2.075 | 394 |

Seismic hazard analyses were run in OpenSHA (Field et al. 2003). The implementation of the UCERF3 model in OpenSHA had been set up to return mean hazard only, i.e., the epistemic uncertainties contained within the model are considered in the analyses, but were not reflected in the output. As part of this work, new capabilities have been developed within OpenSHA to export percentiles of ground motion for a given hazard level using either the UCERF3 or NSHM23 models. No particular distribution is assumed in this process, rather the percentiles reflect the model output for the particular site and the selected ground motion parameter. In the case of the NSHM23 model, the analyses reported here randomly sampled ~10,000 branches from the suite of 121,500 earthquake rupture forecast branches to streamline computations.

The OpenSHA tool was run 2464 times to generate hazard curves for 14 different $V_{S30}$ values, 4 NGA-West2 ground motion models (Abrahamson et al. 2014, Boore et al. 2014, Campbell & Bozorgnia 2014, and Chiou & Youngs 2014), and 22 different oscillator periods at each site. This prototype version of OpenSHA allows for the generation of the hazard curves associated with each logic tree branch of the UCERF3 or the NSHM23 source models. For each run, 16 hazard percentiles with respect to source model uncertainty were generated: 0.1, 1.3, 2.5, 5, 9.25, 16, 33, 50, 67, 84, 90.75, 95, 97.5, 98.7, 99.9, and the mean. This calculation took over two days on 36 computer nodes at the Center for Advanced Computing Research at the University of Southern California. This paper is related to an ongoing effort to parameterize the source epistemic distribution at various

sites across California so that individual practitioners, who may not have access to the computing resources needed to run calculations at this scale, can include uncertainties in their analyses.

## 3.  Source Model Uncertainty

To isolate source model uncertainty, we consider hazard results for a single GMM and single $V_{S30}$ value, and then sample the ground motion distribution for a particular hazard level as described in Section 2. The NSHM23 source model was applied. The results were found to be log-normally distributed based on visual inspection of the corresponding ground motion cumulative distribution functions. Using the python library, SciPy (Virtanen et al., 2020), log normal distributions were fit to all of the ground motion - percentile distributions for 20 return periods, as demonstrated in Figure 2. This standard deviation quantifies source model uncertainty, which is $\sigma_S$=0.053 for the example in Figure 2. This process can be repeated for different GMMs and different $V_{S30}$ values to test sensitivities.
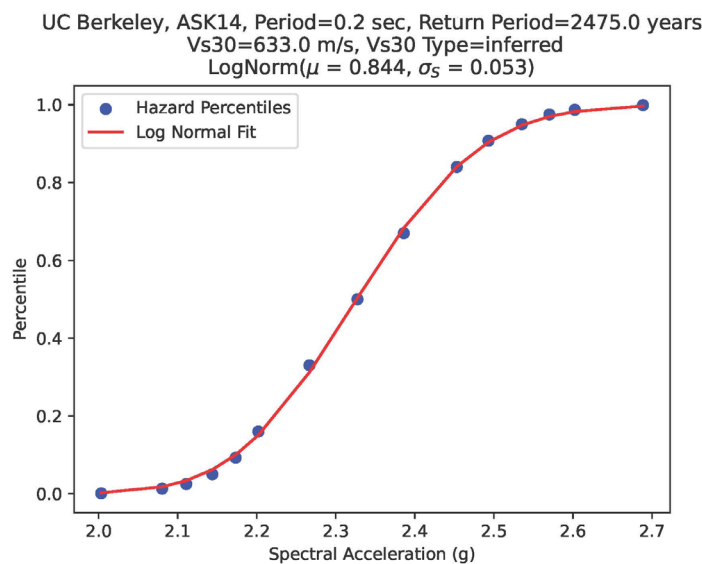


*Figure 2: Source model uncertainty calculation example (NSHM23 source model).*

For each site, oscillator period, and $V_{S30}$ type (measured or inferred), source model uncertainty for each GMM and $V_{S30}$ value combination (28 for each location, oscillator period, and $V_{S30}$ type) were graphed against return period to see general trends and check dependencies. Figure 3 shows these graphs for inferred $V_{S30}$ values for oscillator periods of 0.2 and 1.0 sec at both Berkeley and Davis.

Figure 3 demonstrates that for the shown oscillator periods, source model uncertainty has only modest dependence on GMM and $V_{S30}$ value at Berkeley but is strongly dependent on GMM and $V_{S30}$.at Davis. At Berkeley, source uncertainty gets slightly smaller as return period increases and at Davis, source uncertainty gets slightly larger as return period increases. As expected, mean source uncertainty is higher for the Davis site than for the Berkeley site at all return periods for oscillator periods of 0.2 and 1.0 sec.
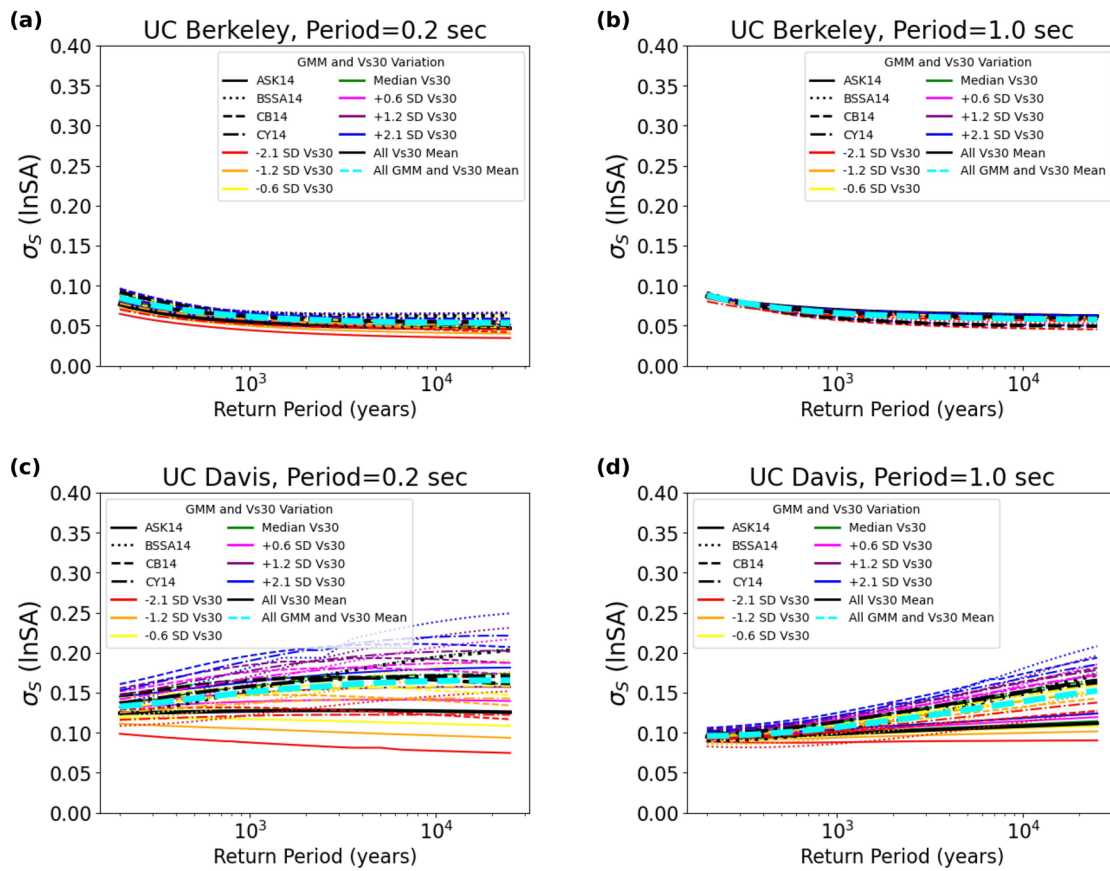
*Figure 3: NSHM23 source model uncertainty vs. return period for every GMM and inferred $V_{S30}$ combination for (a) Berkeley site, 0.2 sec. (b) Berkeley site, 1.0 sec (c) Davis site, 0.2 sec. (d) Davis site, 1.0 sec.*

## 4.  Ground Motion Model Uncertainty

To evaluate GMM uncertainty (i.e., uncertainty in ground motions resulting from alternate GMMs), we consider changes in median hazard (from source uncertainty) across different GMMs for fixed $V_{S30}$ values. This uncertainty was quantified by calculating the standard deviation of the log of the median ground motions from the four NGA-West2 GMMs for each location, oscillator period, and $V_{S30}$ value. For each location, oscillator period, and $V_{S30}$ type, GMM uncertainty for each $V_{S30}$ value (seven for each location, oscillator period, and $V_{S30}$ type) was graphed against return period to see if GMM uncertainty is dependent on $V_{S30}$. Figure 4 shows these graphs for inferred $V_{S30}$ values for oscillator periods of 0.2 and 1.0 sec. at both Berkeley and Davis sites.

Figure 4 demonstrates that for both oscillator periods, GMM uncertainty is nearly independent of $V_{S30}$ at Davis and more strongly dependent on $V_{S30}$ at Berkeley. At both Berkeley and Davis, GMM uncertainty increases with increasing return period. The mean GMM uncertainty value across all return periods is higher at Davis for both oscillator periods of 0.2 and 1.0 sec.
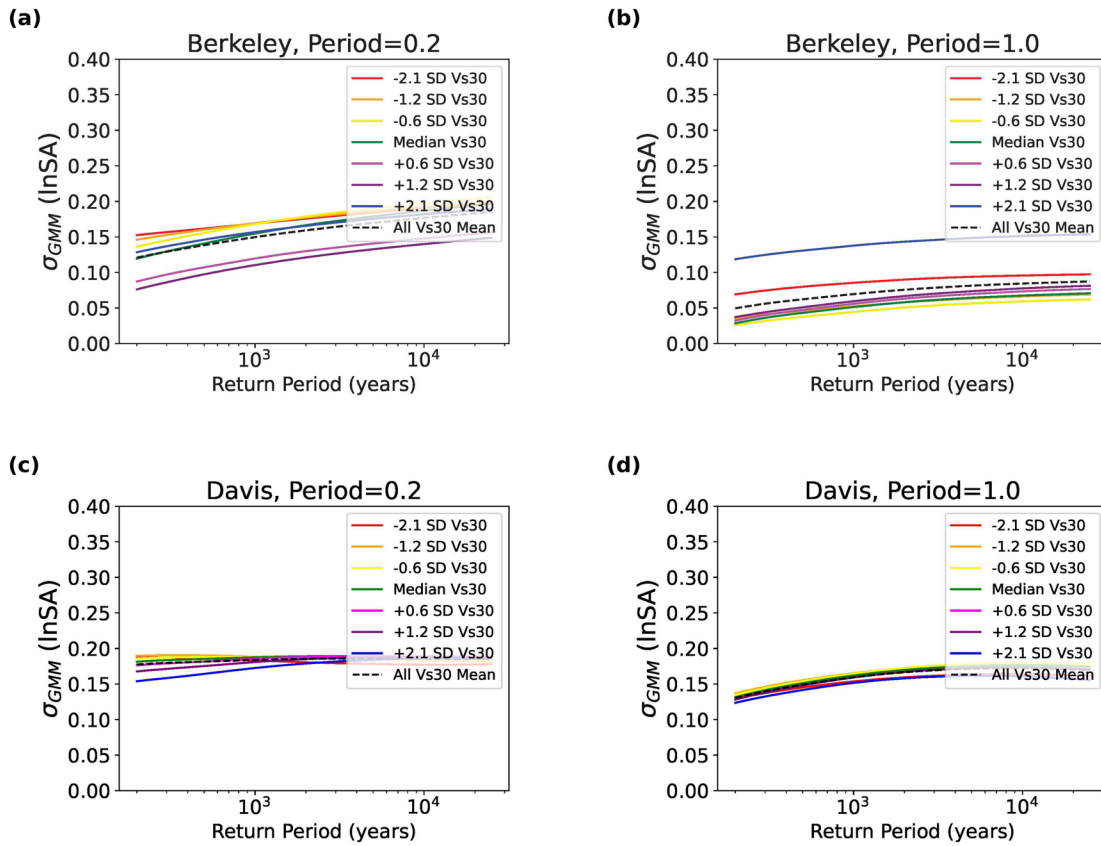
*Figure 4: GMM uncertainty vs. return period for every inferred $V_{S30}$ for (a) Berkeley site, 0.2 sec. (b) Berkeley site, 1.0 sec. (c) Davis site, 0.2 sec. (d) Davis, 1.0 sec.*

## 5. Site Parameter Uncertainty

To evaluate site parameter uncertainty (i.e., uncertainty in ground motions resulting from alternate $V_{S30}$ values), we consider changes in median hazard (from source uncertainty) for a given GMM for a range of $V_{S30}$ values that sample a distribution. Two distribution types are considered, one for measured $V_{S30}$ and one for estimated (inferred) $V_{S30}$; each has the same median for a given site but different natural log standard deviations of $V_{S30}$. For a given GMM, the standard deviation of the natural log of the median ground motions from the seven $V_{S30}$ values was computed for each location, oscillator period, and $V_{S30}$ type. Figure 5 shows results for each site and GMM for the case of measured $V_{S30}$, and Figure 6 shows similar results for the case of inferred $V_{S30}$.

Figure 5 demonstrates that for the Berkeley site at an oscillator period of 0.2 seconds, measured site parameter uncertainty is dependent on GMM. This occurs because different GMMs have different dependencies (i.e., scaling) of site amplification with $V_{S30}$. Figure 6 shows the expected result that site parameter uncertainty is much greater when $V_{S30}$ is inferred instead of measured. Both measured and inferred site parameter uncertainties are greater at Berkeley than Davis. This occurs because the Berkeley site has a large $V_{S30}$, which produces limited nonlinearity, whereas the Davis site is softer and has appreciable nonlinearity. Nonlinearity in the site response is known to decrease the dispersion of ground surface motions (e.g., Stewart et al. 2017). Figure 6 also shows larger site parameter uncertainty at a 1.0 sec. oscillator period than at 0.2 sec. The increased uncertainty at long periods results from stronger $V_{S30}$ scaling as period increases from 0.2 to 1.0 sec.
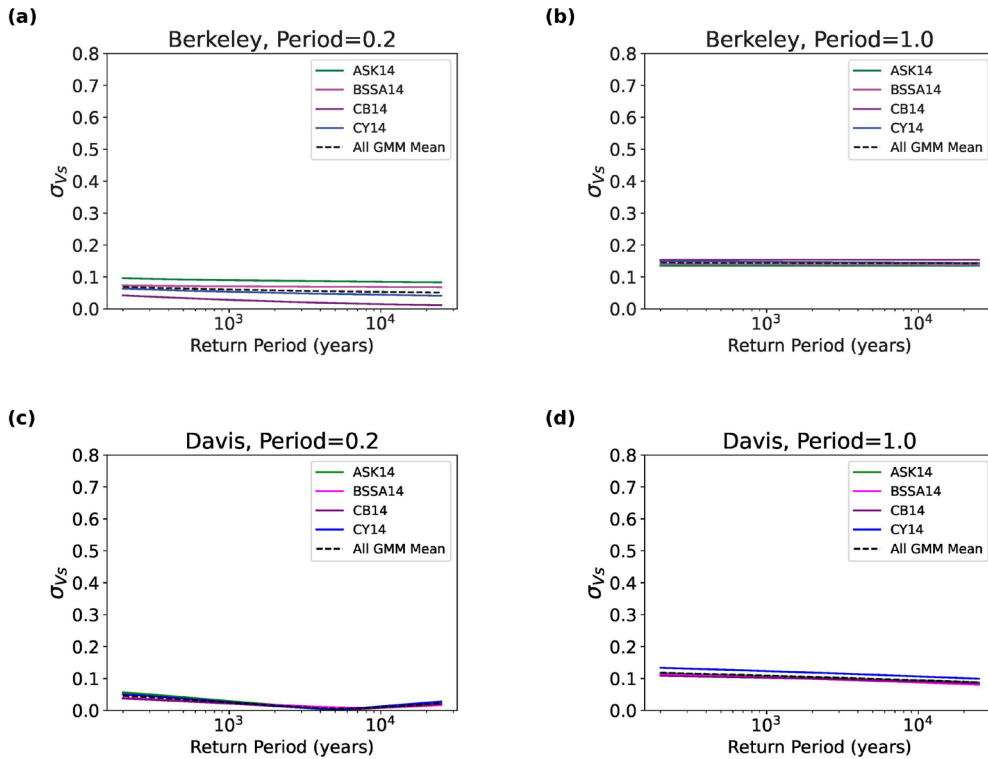
*Figure 5: Site parameter uncertainty vs. return period for V_{S30} distribution associated with measurements for each NGA-West2 GMM for (a) Berkeley site, 0.2 sec (b) Berkeley site, 1.0 sec (c) Davis site, 0.2 sec (d) Davis site, 1.0 sec.*
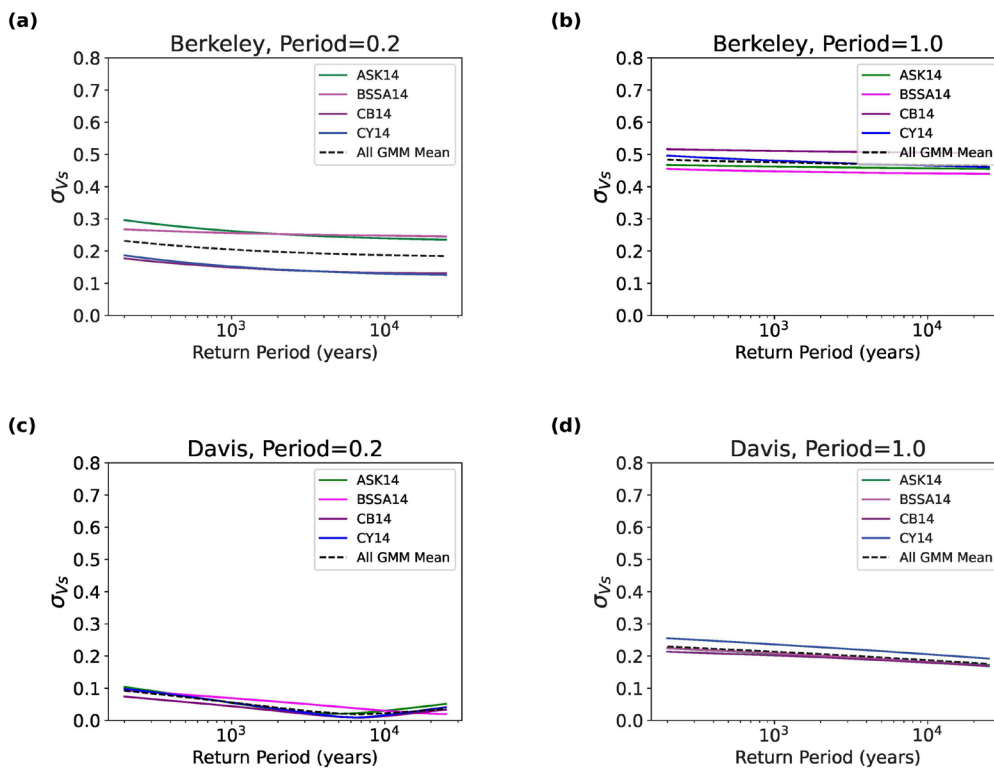


*Figure 6: Site parameter uncertainty vs. return period for V_{S30} distribution associated with estimates for each NGA-West2 GMM for (a) Berkeley site, 0.2 sec (b) Berkeley site, 1.0 sec (c) Davis site, 0.2 sec (d) Davis, 1.0 sec.*

# 6.  Total Epistemic Uncertainty

Total epistemic uncertainty is computed by jointly considering the alternate percentiles representing source uncertainty, the four GMMs, and the 7 $V_{S30}$ values (both for measured and inferred conditions). This combined uncertainty is shown in Figure 7 for the case of an oscillator period of 0.2 seconds at a 2475-year return period for inferred $V_{S30}$ values at the Berkeley site. The cumulative distribution function is well-represented as log-normal with a standard deviation of 0.264. Figure 8 shows the total uncertainty as a function of oscillator period for both sites. Values range from about 0.20 to 0.50 (PGA to 3.0 sec) for the Berkeley site and are about 0.32-0.38 for the Davis site (over the same period range).

We investigated whether the calculation of total epistemic uncertainty could be simplified by considering the source uncertainty independently of the GMM and $V_{S30}$ uncertainty. If this were found to be effective, the total epistemic uncertainty could be calculated using the following equation:

$$\hat{\sigma}_{Total} = \sqrt{\sigma_S^2 + \sigma_{GMM/Vs}^2} \qquad (2)$$

where $\sigma_{GMM/Vs}$ is the combined GMM and site parameter uncertainty, which would not be allowed to drop below the minimum values suggested by Al Atik and Youngs (2014). The reason this hypothesis was tested was because, in concept, $\sigma_S$ values could be evaluated for different regions across the state a priori, and $\sigma_{GMM/Vs}$ could be evaluated for a given site of interest, which requires much less computational cost that jointly considering all three sources of uncertainty.

In addition to total epistemic uncertainty, Figure 8 also shows values of $\hat{\sigma}_{Total}$ using Eq. (2). For the plot in Figure 8, the $\sigma_S$ values were computed for each GMM and $V_{S30}$ and averaged (as variances). The values of $\hat{\sigma}_{Total}$ from Eq. (2) are less than the total epistemic uncertainty ($\sigma_{Total}$) across all periods. This shows that the total uncertainty is underestimated by Eq. (2), although the level of underestimation is small and arguably not significant at Berkeley but larger at Davis.
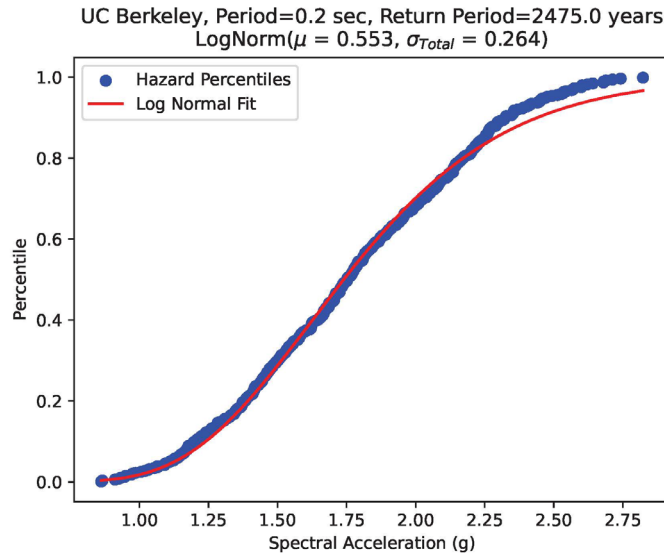


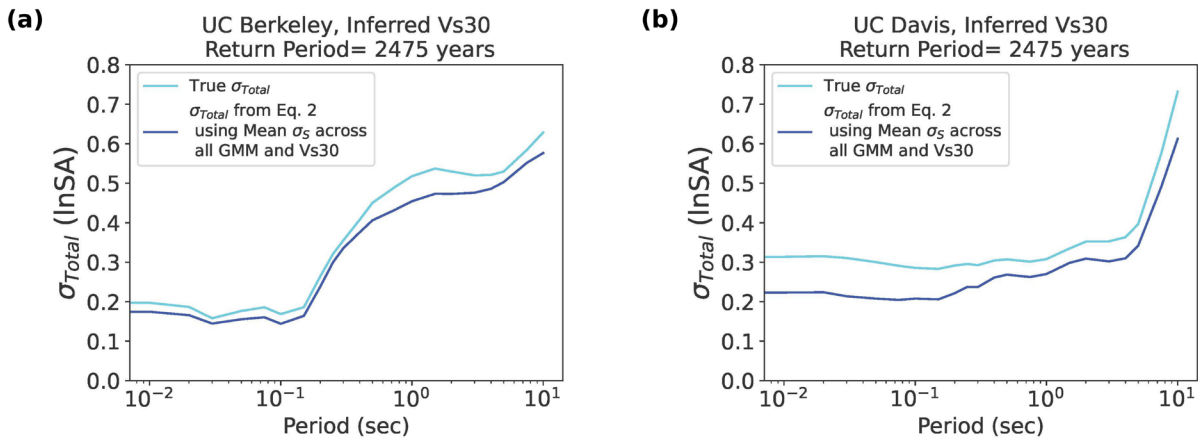*Figure 7: Total epistemic uncertainty for inferred $V_{S30}$ calculation example.*

**(a)**



**(b)**

Figure 8: Total epistemic uncertainty vs oscillator period for inferred $V_{S30}$ at a 2475-year return period for (a) UC Berkeley (b) UC Davis.

## 7. Relative Contributions of Different Sources of Epistemic Uncertainty

To understand the relative contributions of different elements of a PSHA to the total uncertainty, it is useful to examine the individual uncertainties together for a given site and exceedance frequency. This is provided in Figure 9, where we show for the Berkeley and Davis sites the component and total uncertainties as a function of period for a return period of 2475 years. Five uncertainties are shown: source uncertainty computed in the same manner as in Figure 8, combined GMM and $V_{S30}$ uncertainty for the case of measured $V_{S30}$, combined GMM and $V_{S30}$ uncertainty for the case of inferred $V_{S30}$, total uncertainty as calculated in Figure 7 for measured $V_{S30}$ and total uncertainty as calculated in Figure 7 for inferred $V_{S30}$.
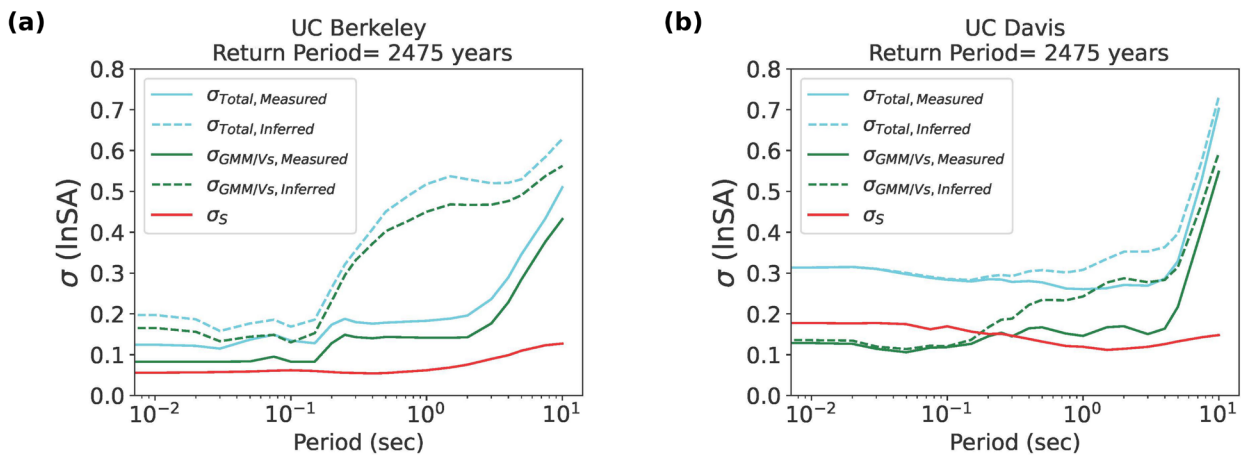
**(a)**



**(b)**

Figure 9: Total and component epistemic uncertainties vs oscillator period at a 2475-year return period for (a) Berkeley site and (b) Davis site.

Figure 9 demonstrates that at both locations and for oscillator periods above approximately 0.2 seconds, the GMM/site parameter uncertainty is larger than the source uncertainty. However, at oscillator periods at or below approximately 0.2 seconds, source uncertainty is higher than GMM / site parameter at Davis and comparable to GMM / site parameter for measured $V_{S30}$ values at Berkeley. At Berkeley, the GMM / site parameter uncertainties grow with period for periods beyond about 0.2-0.3 sec. This likely occurs because of the relatively strong effects of $V_{S30}$-scaling at these longer periods. The strongest contributor to the GMM / site parameter uncertainty is controlled by whether $V_{S30}$ is based on measurement or inference, with the GMMs exerting the largest influence when $V_{S30}$ is measured and the $V_{S30}$-related uncertainty otherwise having the largest influence, particularly at long periods.

Figure 10 shows Uniform Hazard Spectra (UHS) for a 2% probability of exceedance in 50 years (2475 return period) for the Berkeley and Davis sites. Results are shown for two representations of epistemic uncertainty: (1) full uncertainty as described in this paper and (2) partial uncertainty considering GMM and $V_{S30}$ but with source uncertainty only represented through the mean hazard. The second representation is presented because prior to the recent update to OpenSHA, this is the only manner in which uncertainties could practically be considered. For each representation, we show three percentiles (5, 50, 95) and the mean hazard.

**(a)**

UC Berkeley, Inferred Vs30
Uniform Hazard Spectrum
2% Chance of Exceedance in 50 years
(Return Period= 2475 years)

**(b)**

UC Davis, Inferred Vs30
Uniform Hazard Spectrum
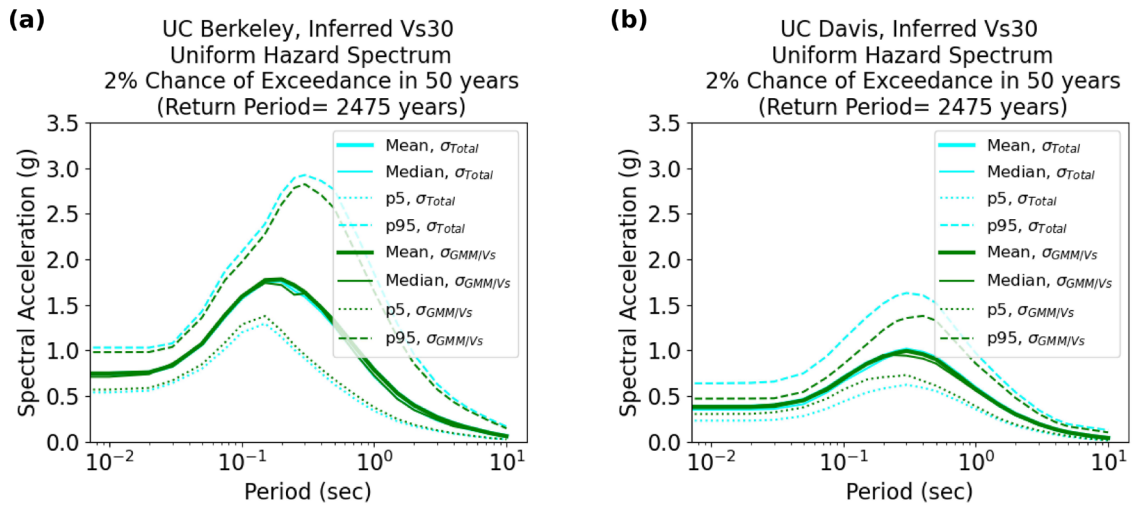2% Chance of Exceedance in 50 years
(Return Period= 2475 years)

*Figure 10: UHS (2475-year return period) with hazard percentiles and mean hazard for two representations of epistemic uncertainty with and without explicit consideration of source uncertainties in percentiles for (a) Berkeley site (b) Davis site.*

The results show that a broader distribution of hazard is obtained when source uncertainties are considered, as expected. The median hazards are nearly the same and the mean hazards match. The match of the mean hazards occurs because source uncertainty is considered in the derivation of the mean hazard in OpenSHA, even before the updates described in Section 2 were implemented.

For all the results presented to this point, the source-related epistemic uncertainty has been based on the model applied in the 2023 update to the National Seismic Hazard Map (NSHM23). This source model (from Field et al. 2023) represents an update to the UCERF3 (Field et al. 2014, 2017), which had been in use for nearly a decade. Repeating the calculations presented previously with the older UCERF3 source model shows a notably smaller impact of source-related uncertainties, as shown in Figure 11 (which matches the form of Figure 9).

**(a)**

UC Berkeley
Return Period= 2475 years

**(b)**

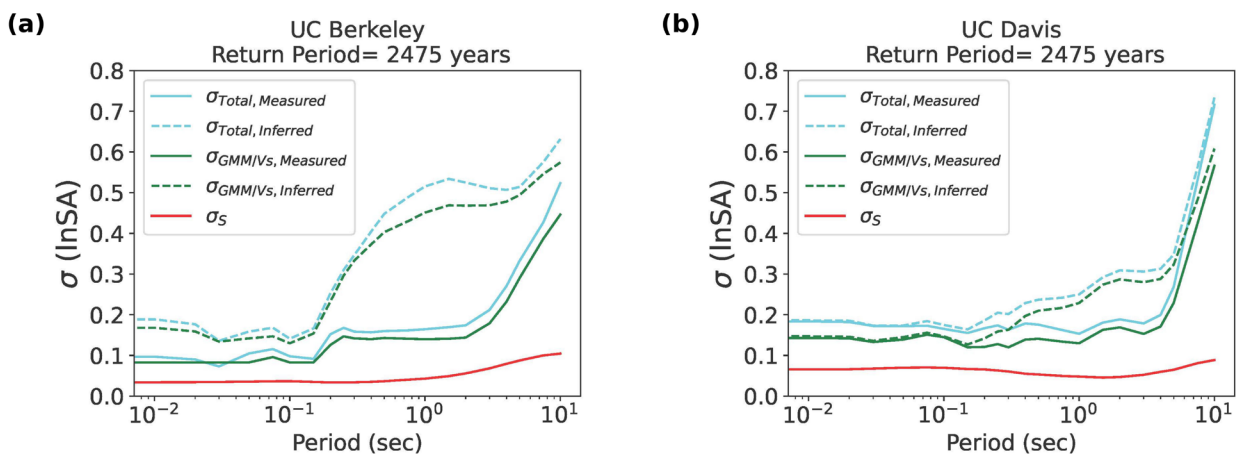UC Davis
Return Period= 2475 years

*Figure 11: Total and component epistemic uncertainties vs oscillator period at a 2475-year return period for (a) Berkeley site and (b) Davis site, now using the UCERF3 source model (Field et al. 2014).*

## 8.  Conclusions

We consider three major sources of epistemic uncertainty in PSHA for California sites, which are seismic source, GMMs, and site parameters. We have adapted OpenSHA to return percentiles representing source uncertainties, which are found to be log-normally distributed and much larger for the Field et al. (2023) source model than the earlier UCERF3 model (Field et al. 2014, 2017). GMM uncertainties are considered by applying multiple models with a lower limit uncertainty from Al Atik and Youngs (2014). Site parameter uncertainties are captured by log-normal distributions of $V_{S30}$, with the spread of the distribution being narrow when $V_{S30}$ is based on measurement and wide when inferred. To illustrate these procedures, we apply the presented framework for sites in Berkeley and Davis. We show that above oscillator periods of about 0.2 sec, combined GMM/site parameter uncertainty is a larger contributor to epistemic uncertainty than source model uncertainty for both measured and inferred $V_{S30}$ values at both locations. However, at oscillator periods below approximately 0.2 sec, source uncertainty is the largest contributor to epistemic uncertainty at Davis. We further show that combined GMM/site parameter uncertainty is most strongly influenced by site parameter uncertainty when $V_{S30}$ is estimated, and by between-model uncertainties when $V_{S30}$ is measured.

We demonstrate that total epistemic uncertainty exceeds the estimates provided by combining source and GMM / site parameter uncertainties under the assumption of independence, although the amount of increase is arguably only significant at the Davis site This indicates that the different uncertainty types are correlated. We will attempt to quantify this correlation in future work.

## Acknowledgments

## 9.  References

Al Atik, L. and Youngs, R. (2014). Epistemic Uncertainty for NGA-West 2 Models. *Earthquake Spectra,* 30(3), 1301-1318.

Bommer, J.J., Scherbaum, F., Bungum, H., Cotton, F., Sabetta, F., and Abrahamson, N. A. (2005). On the use of logic trees for ground-motion prediction equations in seismic hazard analysis, *Bull. Seismol. Soc. Am.* 95 (2) 377–389.

Der Kiureghian, A. and Ditlevsen, O. (2009). "Aleatory or epistemic? Does it matter?," *Structural Safety*, Vol. 31, pp. 105-112.

Faber, M.H. (2005). "On the treatment of uncertainties and probabilities in engineering decision analysis," *Journal of Offshore Mechanics and Arctic Engineering*, Vol. 127, No. 8, pp. 243-248.

Field, EH, RJ Arrowsmith,GP Biasi, P Bird, TE Dawson, KR Felzer, DD Jackson, KM Johnson, TH Jordan, C Madden, AJ Michael, KR Milner, MT Page, T Parsons, PM Powers, BE Shaw, WR Thatcher, RJ Weldon II, and Y Zeng, 2014. Uniform California earthquake rupture forecast, Version 3 (UCERF3)—The Time-Independent Model, *Bull. Seism. Soc. Am.*, 104 (3), 1122–1180.

Field, EH, Jordan TH, Page MT, Milner KR, Shaw BE, Dawson TE, Biasi GP, Parsons T, Hardebeck JL, Michael AJ, Weldon II RJ, Powers PM, Johnson KM, Zeng Y, Felzer KR, Van Der Elst N, Madden C, Arrowsmith R, Werner MJ, and Thatcher WR (2017). A Synoptic View of the Third Uniform California Earthquake Rupture Forecast (UCERF3). *Seismological Research Letters* (2017) 88 (5): 1259–1267.

Field EH, Milner KR, Hatem AE, Powers PM, Pollitz FF, Llenos AL, Zeng Y, Johnson KM, Shaw BE, McPhillips DF, Thompson Jobe JA, Michael AJ, Shen Z-K, Evans EL, Hearn EH, Shumway AM, Mueller CS, Frankel AD, Petersen MD, DuRoss CB, Briggs RW, Page MT, Rubinstein JL and Herrick JA (2023) The USGS 2023 conterminous U.S. time-independent earthquake rupture forecast, Bulletin of the Seismological Society of America, in press.

Field, E.H., T.H. Jordan, and C.A. Cornell (2003). OpenSHA: A Developing Community-Modeling Environment for Seismic Hazard Analysis, *Seismological Research Letters*, 74, no. 4, p. 406-419.

Kwak D.Y., Ancheta T.D., Mitra D., Ahdi S.K., Zimmaro P., Parker G.A., Brandenberg S.J., and Stewart J.P., (2017). Performance evaluation of *VSZ*-to-*VS*30 correlation methods using global *VS* profile database, 730 *Proceedings*, *3rd International Conference on Performance-based Design in Earthquake Geotechnical* 731 *Engineering (PBD-III)*, Paper No. 399, Vancouver, Canada

Kwak DY, Ahdi SK, Wang P, Zimmaro P, Brandenberg SJ, Stewart J.P. (2021). Web portal for shear wave velocity and HVSR databases in support of site response research and applications. UCLA Geotechnical Engineering Group. DOI:10.21222/C27H0V

McGuire, R.K. (2004). *Seismic hazard and risk analysis*, EERI Monograph MNO-10, *Earthquake Engineering Research Institute*, Oakland, CA, 187 pp.

McGuire, R.K., Cornell, C.A., and Toro, G.R. (2005). The case for the mean hazard curve," *Earthquake Spectra*, Vol. 21, pp. 879-886

Miller A.C. and Rice T.R. (1983). Discrete Approximations of Probability Distributions, *Management Science,* 29(3)

Milner, K.R. and Field, E.H. (2023). A Comprehensive Fault System Inversion Approach: Methods and Application to NSHM23, Bulletin of the Seismological Society of America, in press.

Pate-Cornell, M.E. (1996). "Uncertainties in risk analysis: Six levels of treatment," *Reliability Engineering and System Safety,* Vol. 54, No. 2-3, pp. 95-111.\

Stafford, P.J. (2015). "Variability and uncertainty in empirical ground-motion prediction for probabilistic hazard and risk analyses," Chapter 4 in *Perspectives on European Earthquake engineering and Seismology,* A. Ansal (ed.), pp. 97-128.

URS Corporation (2015). 2015 update to the site-specific seismic hazard analyses and development of seismic design ground motions University of California Berkeley.

Waldhauser, F. and Ellsworth, W. (2002). Fault Structure and Mechanics of the Hayward Fault, California, from double-difference earthquake locations. *Journal of Geophysical Research*, Vol. 107, No. B3

Virtanen, P., Gommers, R., Oliphant, T. E., Haberland, M., Reddy, T., Cournapeau, D., … SciPy 1.0 Contributors. (2020). SciPy 1.0: Fundamental Algorithms for Scientific Computing in Python. *Nature Methods*, *17*, 261–272. https://doi.org/10.1038/s41592-019-0686-2

Wills, C., Gutierrez, C., Perez, F., Branum, D. (2015). A Next Generation VS30 Map for California Based on Geology and Topography. *Bulletin of the Seismological Society of America*, Vol. 105, No. 6